The 34th International Workshop on Water Waves and Floating Bodies, Newcastle, NSW, Australia, April 7 - 10, 2019

Gap resonance driven by linear, quadratic and cubic wave excitation

W. Zhao[a,*], P. H. Taylor[a], H.A. Wolgamot[a], R. Eatock Taylor[b]

[a] Faculty of Engineering and Mathematical Sciences, The University of Western Australia, 35 Stirling Highway, Crawley, WA, 6009 Australia. *E-mail: wenhua.zhao@uwa.edu.au

[b] Department of Engineering Science, University of Oxford, Oxford, OX1 3PJ, UK

Highlights

- Resonant fluid responses in the gap between two identical fixed rectangular boxes are experimentally investigated for uni-directional transient wave groups with broadside incidence;
- The surface elevations at the centre of the gap (the so-called gap resonance) can be excited both linearly and nonlinearly, e.g. through frequency-doubling and frequency-tripling processes;
- The time histories of the nonlinearly excited gap resonances are remarkably similar to that from linear excitation;
- The sum-frequency transfer functions for gap surface elevations must then depend strongly on the output sum frequency, but only weakly on the differences between the interacting linear components.

1. Introduction

Fluid resonant response in a narrow gap (so called gap resonance) is a weakly damped phenomenon, which may occur between two side-by-side vessels in close proximity where waves cannot efficiently radiate outwards from the narrow gap. The mode shapes and frequencies of the gap resonances can be well approximated with the potential flow analysis of Molin et al. (2002, 2018). Considerable effort has also focused on the estimation of the response amplitudes, e.g. by introducing different methods to account for viscous damping (e.g. Chen, 2005 and Faltinsen & Timokha, 2015) or nonlinearity in the free-surface boundary conditions.

Much work has looked at linear excitation, where the incoming wave frequency is close to that of the gap resonance. However, gap resonances driven through nonlinear processes are also of practical interest, as the gap resonance frequencies can be substantially higher than those of the incident waves for narrow gaps typical of LNG transfer operations from a FLNG facility. A comprehensive study of gap resonance was made by Sun et al. (2010) using potential flow diffraction theory at first and second order. In a large wave basin, Zhao et al. (2017) successfully excited the gap resonance through a frequency-doubling process, and found that the second harmonic of the gap resonance could be as large as the linear response component.

There are some important open questions remaining on the excitation mechanism of the gap resonance phenomenon, e.g. (1) whether gap resonance can be driven by a frequency-tripling process; (2) if so, how the gap resonance will behave. A series of tank tests under NewWave-type (Jonathan and Taylor, 1997) wave groups help us to address these questions. Gap resonances driven through different mechanisms (e.g. linear or nonlinear excitations) are investigated. The normalized time history of the gap resonance driven through frequency tripling agrees extremely well with that driven by frequency doubling, and both are similar to the response due to linear excitation.

2. Experimental set-up

The experiments were performed in the Deepwater Wave Basin at Shanghai Jiao Tong University. The wave basin is 50 m long, 40 m wide and the water depth was set to 10 m. Flap-hinged wavemakers are fixed along two neighbouring sides of the basin and wave absorbing beaches are installed on the opposite sides to minimize reflected waves.

The experimental set-up is the same as in Zhao et al. (2017), where tests focused on the resonant fluid responses and the corresponding damping in a narrow gap. Two identical 3.333 m long and 0.767 m wide rectangular boxes were used, these were 0.425 m high and immersed such that the undisturbed draught was 0.185 m. The two boxes were rigidly mounted to a gantry near the centre of the wave basin in a side-by-side configuration, forming a narrow gap of 0.067 m (see figures 1 & 2 in Zhao et al. 2017). Slightly different to Zhao et al. (2017), the two boxes in this study are fixed in the middle of the basin, e.g. the centre of the gap is 25.46 m away from the paddle and about 25 m from the wave absorber. This is to maximize the measurement window before reflected waves arrive from the paddles, downstream absorbers or side walls. Focusing on the resonant surface elevations in the gap, we use uni-directional transient wave groups broadside onto the boxes. The undisturbed wave field was calibrated in the absence of the models. With the models in place, the same paddle signal was then used to generate identical incident wave conditions.

Three sets of transient wave groups are generated based on Gaussian spectra, with the spectral peak frequency being $f_P = f_{m=1}$ for the first set, $2\text{x}f_P = f_{m=1}$ for the second and $3\text{x}f_P = f_{m=1}$ for the third, where $f_{m=1} = 1.025$ Hz is the frequency of the first resonant mode with one half-wavelength along the gap (Zhao et al. 2017). The maximum linearized surface elevation at the wave gauge at the gap centre but without the boxes present is measured to be 25 mm for the first set, 48 mm for the second set and 148 mm for the third set. It should be noted that the exact value of the maximum surface elevation is not important here, as we are interested in the shapes in time of the response profiles. Each set of the transient wave group tests included running the same signal with four different phase angles, i.e. 0º, 90º, 180º and 270º, to allow for a complete extraction of the harmonic components for the gap resonance, as in Fitzgerald et al. (2014) and Zhao et al. (2017).

3. Spectral analysis of the measured signals in the basin

Time histories of the surface elevations were sampled at 40 Hz, with and without the model in the basin. In this study, we obtain three sets of undisturbed (η) and response (φ) time histories, with each set consisting of crest-focused (0º), up-crossing (90º), trough-focused (180º) and down-crossing (180º) signals. For simplicity, we use the crest-focused (0º) signal as representative for both η and φ. The amplitude spectra of the undisturbed and response surface elevations for the three sets of tests are shown in Fig. 1, where the subscripts 1x, 2x and 3x represent the excitation mechanisms.

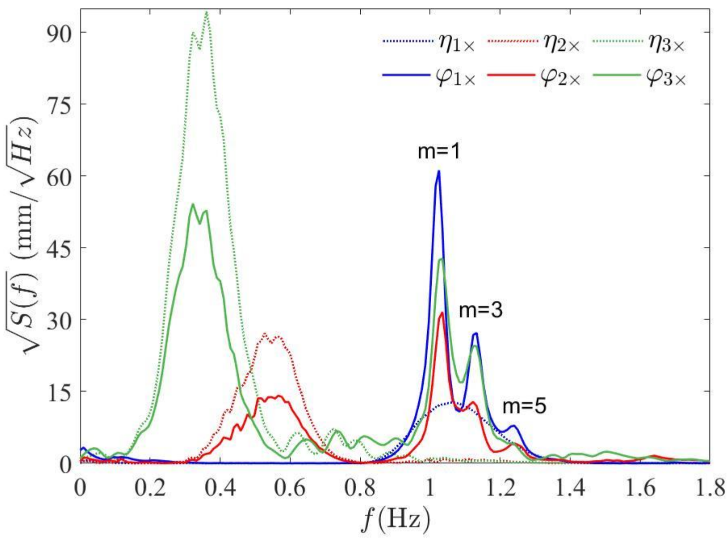

Fig. 1 Amplitude spectra of the surface elevations at the centre of the gap with and without the model in place. The dotted lines represent the undisturbed waves (η) in the absence of the model, while the solid lines are the response surface elevations (φ) measured with the model in place using the same wave gauge at the same location. The subscripts 1x, 2x and 3x in the undisturbed and response surface elevations denote the cases for incoming waves with spectral peak frequency $f_P = f_{m=1}$, $2\text{x}f_P = f_{m=1}$ and $3\text{x}f_P = f_{m=1}$, respectively.

The spectra of the undisturbed incoming waves (dotted lines) show little nonlinearity in Fig. 1. Large amplitude responses at the first few gap resonance modes are excited in the linear (1x) case (blue curve), which is not surprising. The most striking observation from Fig 1 is that significant surface elevations at the gap resonance modes have been excited in the 2x (red curve) and 3x (dark green curve) cases, much higher in frequency than the main incident wave components. Thus, they are driven through frequency-doubling and frequency-tripling processes, where the output sum frequencies are close/equal to the natural frequencies of the first few gap resonance modes. This is demonstrated in the following section.

4. Time histories driven through linear excitation, frequency doubling and tripling

Four-phase decomposition is conducted as in Zhao et al. (2017), separating the measured surface elevations into the first four harmonics, i.e. terms with frequencies close to ω, 2ω, 3ω and 4ω. The separated harmonics are shown in Fig. 2, though the 3rd and 4th harmonics of η and the 4th harmonic of φ are negligible and thus not shown.

The undisturbed and response surface elevations have been aligned in time as shown in Fig. 2, with $t = 0$ s as the time when the undisturbed wave components focus at the location of the wave gauge (also the centre of the gap when the model is in place). Small second-order error waves can be seen in $\eta_{3\times}^{2+}$ in Fig. 2 (c), which induced some small second-order response. In general, the high harmonics of the undisturbed incoming waves are negligible. In the linear excitation case as shown in Fig. 2 (a), the linear response component (solid blue curve) dominates, while the high harmonics are negligible. In the quadratic excitation case in Fig. 2 (b), the 2nd harmonic response (solid red curve) is as large as the linear component (solid blue curve), while the 3rd response harmonic is small. In the cubic excitation case in Fig. 2 (c), significant 3rd harmonic response (solid dark green curve) is excited. The gap resonances, no matter how they have been driven, e.g. linearly ($\varphi_{1\times}^{1}$), quadratically ($\varphi_{2\times}^{2+}$) and cubically ($\varphi_{3\times}^{3+}$), show very similar profiles in time – decaying slowly with similar beating patterns. The slowly decaying process is associated with the low (radiation+viscous) damping for narrow gaps. The beating pattern is a simple combination of the first three gap resonance modes as shown in Fig. 1 (only odd modes are excited due to the symmetric set-up in experiments).

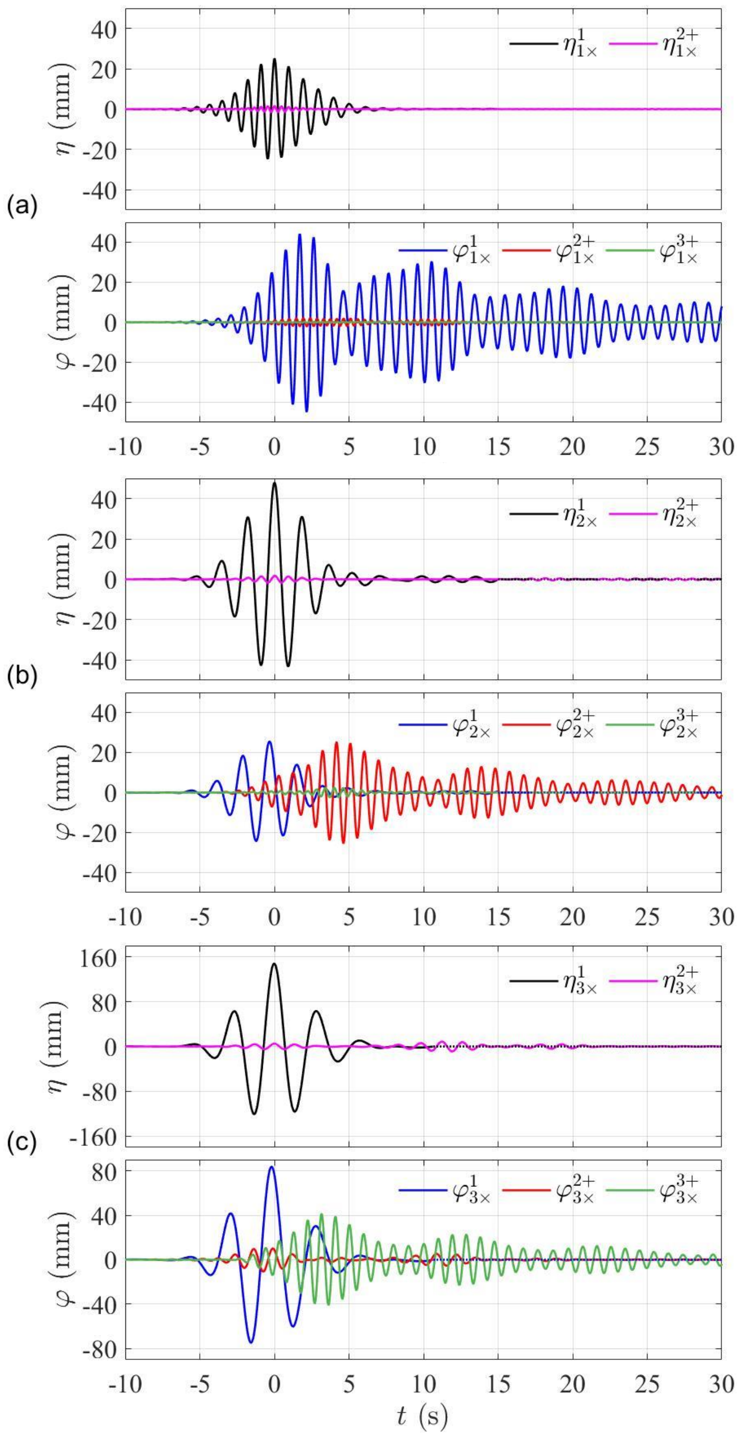

Fig. 2 Harmonics of the undisturbed (η) and response (φ) surface elevations driven by different mechanisms. (a) linear excitation (1x) set; (b) quadratic excitation (2x) set; (c) cubic excitation (3x) set. The superscripts 1, 2+ and 3+ refer to the linear, second and third harmonics, while the subscripts 1x, 2x and 3x represent the different excitation mechanisms.

To explore the similarity of the gap resonances driven by different mechanisms, we plot the normalised (by their maxima) time histories on top of each other in Fig. 3. It is worth mentioning that the time histories are shifted so as to be aligned at the response peak (i.e. $t = 3.15$ s), this is understandable given that they are driven through different processes. The linearly excited signal $\varphi^1_{1\times}$ is heavily shifted in time, aiming to reduce the effect of the linearly driven responses whose frequencies are close to that of the gap resonance modes. This effect could well explain the good but less satisfactory agreement with the gap resonances driven through frequency-doubling ($\varphi^{2+}_{2\times}$) and -tripling ($\varphi^{3+}_{3\times}$) processes. The most striking observation from Fig. 3 is that the gap resonances driven by frequency doubling ($\varphi^{2+}_{2\times}$) agrees extremely well with those by frequency tripling ($\varphi^{3+}_{3\times}$). The agreement shown in Fig. 3 suggests that the sum-frequency transfer functions of the surface elevations in the gap are strongly dependent on the output sum frequency $\sum_{i=1}^{N} \omega_i$, where $N = 2\ or\ 3, \ldots$ but only weakly on frequency difference values, as discussed previously for 2nd harmonic resonances between the legs of multi-column structures (Grice et al. 2015 and Taylor et al. 2007).

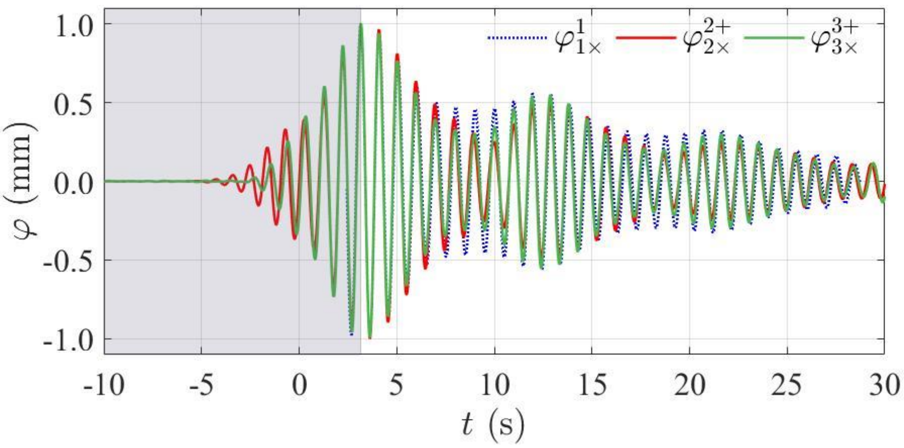

Fig. 3 Normalised gap resonances driven by different mechanisms, i.e. linear excitation ($\varphi^1_{1\times}$), quadratic excitation ($\varphi^{2+}_{2\times}$) and cubic excitation ($\varphi^{3+}_{3\times}$). Note the signals $\varphi^{2+}_{2\times}$ and $\varphi^1_{1\times}$ have been shifted towards the left by 1 s and 16.2 s respectively, to align with the signal $\varphi^{3+}_{3\times}$ at the response peak. The large time shift in $\varphi^1_{1\times}$ is to reduce as much as possible the effect of the linear responses whose frequencies are close to that of the gap resonance modes.

Concluding remarks

Conducting a series of tests with various input Gaussian wave groups, significant gap resonance phenomena have been excited successfully through different mechanisms, i.e. linear excitation, frequency doubling and frequency tripling. We believe the significant resonant fluid response driven by frequency tripling may be a new observation for wave-structure interactions. This phenomenon is somewhat similar to frequency upshifting for light in laser physics (see for example Craxton 1991). The frequency doubling and tripling phenomena may be of practical importance for offshore operations involving vessels with narrow gaps and long period incident swell waves.

No matter whether the gap resonances are driven linearly or nonlinearly, they behave in a similar way once the resonant motions are excited. This requires that the sum frequency transfer functions of the gap resonance significantly depend on the output sum frequency. The sum frequency $(\omega_1 + \omega_2)$ surface QTFs then have a 'near-flat' structure in the direction perpendicular to the leading diagonal - a similar empirical form to the Newman approximation (1974) for difference frequency $(\omega_1 - \omega_2)$ force QTFs for vessels in irregular waves, but here for sum frequencies. Cubic sum transfer functions for the gap must have comparable structure. Further evidence for this will be presented at the workshop.

Acknowledgement

The first author is grateful for the DECRA fellowship (DE190101296) awarded by Austrlian Research Council.

References

Chen, X.B., 2005. Hydrodynamic analysis for offshore LNG terminals. *In Proceedings of the 2nd International Workshop on Applied Offshore Hydrodynamic*s, Rio de Janeiro.

Craxton, R.S. 1991. High efficiency frequency tripling schemes for high power Nd:glass lasers. *IEEE J. Quantum. Electron.* 1771-82.

Faltinsen, O.M. & Timokha, A.N., 2015. On damping of two-dimensional piston-mode sloshing in a rectangular moonpool under forced heave motions. *Journal of Fluid Mechanics*, 772, R1.

Fitzgerald, C., Taylor, P.H., Eatock Taylor, R., Grice, J.R. and Zang, J. 2014. Phase manipulation and the harmonic components of ringing forces on a surface-piercing column. *Proc. Roy. So. A*, 470, no. 2168 20130847.

Grice, J.R., Taylor, P.H., Eatock Taylor, R., Zang, Z. and Walker, D.A.G. 2015. Extreme free surface elevations beneath offshore platforms, 2nd order trapping, and the near flat form of the quadratic transfer functions. *Computers and Fluids*, 119, 13-25.

Jonathan, P., Taylor, P.H., 1997. On irregular, nonlinear waves in a spread sea. *J. Offshore Mech. Arct. Eng.*, 119, 37-41.

Molin, B., Remy, F., Kimmoun, O., Stassen, Y., 2002. Experimental study of the wave propagation and decay in a channel through a rigid ice-sheet. *Applied Ocean Research*, 24 (5), 247–260.

Molin, B., Zhang, X., Huang, H., Remy, F., 2018. On natural modes in moonpools and gaps in finite depth. *Journal of Fluid Mechanics*, 840, 530-554.

Newman, J.N., 1974. Second-order, slowly-varying forces on vessels in irregular waves. *Int. Symp. Dynamics of Marine Vehicle and Structures in Waves*, London, 1974, ed. Bishop, R.E. and Price, W.G.

Sun, L., Eatock Taylor, R., Taylor, P.H., 2010. First- and second-order analysis of resonant waves between adjacent barges. *Journal of Fluids and Structures*, 26 (6), 954–978.

Taylor PH, Zang J, Walker DAG, Eatock Taylor R. 2007 Second order near-trapping for multi-column structures and near-flat QTFs. *22nd IWWWFB*, Croatia. http://www.iwwwfb.org/Abstracts/iwwwfb22/iwwwfb22_48.pdf.

Zhao, W., Wolgamot, H. A., Taylor, P. H., Eatock Taylor, R., 2017. Gap resonance and higher harmonics driven by focused transient wave groups. *Journal of Fluid Mechanics*, 812, 905-939.